

Improved Direct Measurement of A_b and A_c at the Z^0 Pole Using a Lepton Tag*

The SLD Collaboration**

Stanford Linear Accelerator Center
Stanford University, Stanford, CA 94309

Abstract

The parity violation parameters A_b and A_c of the $Zb\bar{b}$ and $Zc\bar{c}$ couplings have been measured directly, using the polar angle dependence of the polarized cross sections at the Z^0 pole. Bottom and charmed hadrons were tagged via their semileptonic decays. Both the electron and muon analyses take advantage of new multivariate techniques to increase the analyzing power. Based on the 1993-98 SLD sample of 550,000 Z^0 decays produced with highly polarized electron beams we measure $A_b = 0.919 \pm 0.030_{stat} \pm 0.024_{syst}$, and $A_c = 0.583 \pm 0.055_{stat} \pm 0.055_{syst}$.

Submitted to Physical Review Letters

* Work supported in part by Department of Energy contract DE-AC03-76SF00515

Parity violation in the $Zf\bar{f}$ coupling can be measured via the observables $A_f = 2v_f a_f / (v_f^2 + a_f^2)$, where v_f and a_f represent the vector and axial vector couplings to fermion f . In particular, for $f = b$, A_b is largely independent of propagator effects that modify the effective weak mixing angle, and thus provides an unambiguous test of the Standard Model.

The Born-level differential cross section for the process $e^+e^- \rightarrow Z^0 \rightarrow f\bar{f}$ is

$$d\sigma_f / dz_f \propto (1 - A_e P_e)(1 + z_f^2) + 2A_f(A_e - P_e)z_f, \quad (1)$$

where P_e is the e^- beam longitudinal polarization ($P_e > 0$ for right-handed (R) polarization) and z_f is the cosine of the polar angle of the outgoing fermion with respect to the incident electron. The ability to modulate the sign of P_e allows the final-state quark coupling A_f to be extracted independently of A_e from a fit to the differential cross section. Thus, the measurements of A_f described here are unique, and complementary to other electroweak measurements performed at the Z^0 pole [1].

This Letter reports the results of the 1996-98 SLD lepton tag analysis, for which identified electrons and muons were used to tag the flavor of the underlying heavy quark. The data sample used in this analysis is roughly three times larger than that of previously reported results [2]. Further statistical and systematic advantage is provided by improvements to the data analysis which take advantage of the precise information provided by the new vertex detector (VXD3) [3] that was installed just prior to the 1996 data run.

The Stanford Linear Collider (SLC) and its operation with a polarized electron beam have been described elsewhere [4]. During the 1996-98 run, the SLC Large Detector (SLD) [5] recorded an integrated luminosity of 14.0 pb^{-1} at a mean center of mass energy of 91.24 GeV, with a luminosity-weighted electron beam polarization of $|P_e| = 0.7336 \pm 0.0038$.

Charged particle tracks are reconstructed in the Central Drift Chamber (CDC) and the CCD-based vertex detector in a uniform axial magnetic field of 0.6T. For the 1996-98 data, the combined $r\phi$ (rz) impact parameter resolution of the CDC and VXD3 is 7.7 (9.6) μm at high momentum, and 34 (34) μm at $p_\perp \sqrt{\sin\theta} = 1 \text{ GeV}/c^2$, where p_\perp is the momentum transverse to the beam direction. The Liquid Argon Calorimeter (LAC) measures the energy

and shower profile of charged and neutral particles with an electromagnetic energy resolution of $\sigma_E/E = 15\%/\sqrt{E(\text{GeV})}$ and is used in the electron identification. The Warm Iron Calorimeter (WIC) detects charged particles that penetrate the 3.5 interaction lengths of the LAC and magnet coil. The Cherenkov Ring Imaging Detector (CRID) measures the velocity of charged tracks in the region $|\cos\theta| < 0.68$ using the number and angle of Cherenkov photons emitted in liquid and gaseous radiators; electrons are well separated from pions in the region between 2 and 5 GeV/c, while pion (kaon) rejection reduces backgrounds to the muon sample in the region $2 < p < 5$ ($2 < p < 15$) GeV/c.

The axis of the jet nearest in angle to the lepton candidate is used to approximate z , the cosine of the polar angle of the underlying quark. Jets are formed from calorimeter energy clusters (including any associated with the lepton candidate) using the JADE algorithm [6] with parameter $y_{cut} = 0.005$. The analyses presented here make substantial use of ‘secondary’ decay vertices which are displaced from the primary interaction point, identified via the ZVTOP topological vertexing algorithm [7], as well as the invariant mass of the tracks comprising the secondary vertex (‘vertex mass’), corrected to account for unmeasured neutral particles [8].

The selection of electron and muon candidates with $p > 2$ GeV/c in hadronic Z^0 decays has been described previously [2]. Electrons are identified with both LAC and CRID information for CDC tracks in the angular range $|\cos\theta| < 0.72$. Electrons from photon conversions are recognized and removed with 73% efficiency. WIC information is also included for muons, providing an essential measurement of their penetration. Muons are identified in the angular region $|\cos\theta| < 0.70$, although the identification efficiency falls rapidly for $|\cos\theta| > 0.60$ due to the limited angular coverage of the WIC. To reduce backgrounds from misidentification and the decay of light hadrons, the 29% of events containing electron candidates that had no reconstructed secondary vertices were removed from the sample, precluding the use of the electron sample for the measurement of A_e .

For $p > 2$ GeV/c, Monte Carlo (MC) studies indicate efficiencies (purities) of 64% (64%) and 81% (68%) for the electron and muon samples, respectively, where the remaining

electrons from photon conversion account for 5% of the 12862 electron candidates. In the case of the muon sample (21199 candidates), the background is due both to misidentification (8% of muon candidates) and to real muons from light hadron decays (25%). In both cases, the MC simulation has been verified with a control sample of pions from $K_S^0 \rightarrow \pi^+\pi^-$ decays. The fraction of such pions misidentified as electrons is $(1.02 \pm 0.06)\%$, consistent with the MC expectation of $(1.06 \pm 0.03)\%$. For muons, the measured pion misidentification fraction is $(0.342 \pm 0.028)\%$, somewhat higher than the MC expectation of $(0.279 \pm 0.012)\%$. This difference has been accounted for by raising the background level in the maximum likelihood fit to the muon sample by $(20 \pm 10)\%$ of itself.

The sample of events containing identified leptons is composed of the following event types (charge conjugates implied): $Z^0 \rightarrow b\bar{b}, b \rightarrow l$ (' bl '); $Z^0 \rightarrow b\bar{b}, b \rightarrow \bar{c} \rightarrow l$ (' $b\bar{c}l$ '); $Z^0 \rightarrow b\bar{b}, \bar{b} \rightarrow \bar{c} \rightarrow l$ (' $\bar{b}\bar{c}l$ '); $Z^0 \rightarrow c\bar{c}, \bar{c} \rightarrow l$ (' $\bar{c}l$ '); and background from light hadron and vector meson decays, photon conversions, and misidentified hadrons (' bk ').

Identification of electron candidate event types is based on the values of eight discriminating variables [9]: track momentum (p), momentum transverse to the nearest jet (p_t), the estimate of the underlying B hadron boost [10] and when available, same hemisphere secondary vertex mass, opposite hemisphere vertex mass, same hemisphere vertex momentum resultant, same hemisphere vertex significance (separation D between the interaction point and secondary vertex, divided by its uncertainty), and L/D (where L is the distance from the interaction point to the point on the secondary vertex trajectory closest to the electron candidate trajectory). These variables are used as inputs to an Artificial Neural Network with three output nodes N_{bl} , $N_{b\bar{c}l}$, and $N_{\bar{c}l}$, optimized for the bl , $b\bar{c}l + \bar{b}\bar{c}l$, and $\bar{c}l$ signals, respectively. Event types are estimated according to the composition of MC electron candidate events with similar output node values. The measured and simulated distributions of the three output node variables are compared in Figure 1.

The Neural Network is trained on the SLD MC sample of hadronic Z^0 decays, generated with JETSET 7.4 [11]. Semileptonic decays of B mesons are generated according to the ISGW formalism [12] with a 23% D^{**} fraction, while semileptonic decays of D mesons are

simulated according to branching ratios reported by the Particle Data Group [13]. Experimental constraints are provided by the $B \rightarrow l$ and $B \rightarrow D$ inclusive momentum spectra measured by the CLEO collaboration [14,15] and the $D \rightarrow l$ momentum spectrum measured by the DELCO collaboration [16]. The detailed simulation of the SLD detector response has been realized using GEANT [17].

Muon candidate event types are estimated according to the composition of MC muon candidate events with similar values of the following discriminating variables [18]: p , p_t , and, when available, L/D and M_{max} , the largest of the secondary vertex invariant masses. The measured and simulated distributions of these variables are compared in Figure 2.

A maximum likelihood analysis of all selected hadronic Z^0 events containing lepton candidates is used to determine A_b and A_c . The likelihood function contains the following probability term for each lepton, with measured charge sign Q :

$$P(P_e, z; A_b) \propto \left\{ (1 + z^2)(1 - A_e P_e) - 2Q(A_e - P_e) \left[(f_b(1 - 2\bar{\chi}_b) - f_{\bar{b}\bar{c}}(1 - 2\bar{\chi}_{\bar{b}\bar{c}}) + f_{b\bar{c}}(1 - 2\bar{\chi}_{b\bar{c}}))(1 - \Delta_{QCD}^b(z))A_b - f_c(1 - \Delta_{QCD}^c(z))A_c + f_{bk}A_{bk} \right] z \right\}. \quad (2)$$

The lepton source fractions f_b , $f_{\bar{b}\bar{c}}$, $f_{b\bar{c}}$, f_c , and f_{bk} , where $\bar{b}\bar{c}$ ($b\bar{c}$) refers to $\bar{b} \rightarrow \bar{c} \rightarrow l$ ($b \rightarrow \bar{c} \rightarrow l$), are functions of the three neural net output node values (electron candidates) or the four discriminating variables (muon candidates). Correction factors $(1 - 2\bar{\chi}_x)$, where χ_x is the mixed fraction for lepton source x , are applied to b-quark lepton sources to account for asymmetry dilution due to $B^0\bar{B}^0$ mixing. The value of $\bar{\chi}_b$ is taken from LEP measurements of the average mixing in semileptonic B decays [1], and is corrected to take into account selection and fitting bias [9,18], including that due to the enhanced likelihood for bcl cascade leptons to have come from a B meson which has mixed.

The asymmetry in the background A_{bk} is parameterized as a function of p and p_t . For the electron sample, the parameterization is determined from tracks in the data not identified as leptons. For the muon sample, MC studies indicated a substantial difference between the true background asymmetry and that of non-leptonic tracks, and so the background asymmetry parameterization was determined directly from the MC simulation.

A z -dependent correction factor $(1 - \Delta_{QCD}^f(z))$ is included in the likelihood function to incorporate the effects of gluon radiation. Calculation of the quantity $\Delta_{QCD}^f(z)$ has been performed by several groups [19]. For an unbiased sample of $b\bar{b}$ or $c\bar{c}$ events with $|z| < 0.7$, correcting for this effect increases the measured asymmetry by $\sim 3\%$ overall. However, a MC simulation of the analysis chain indicates that biases which favor $q\bar{q}$ events over $q\bar{q}g$ events mitigate the effects of leading order gluon radiation by about 30%. Effects due to gluon splitting to $b\bar{b}$ and $c\bar{c}$ have been estimated by rescaling the JETSET simulation to world average gluon splitting measurements [20]. Additional radiative effects, such as those due to initial-state radiation and γ/Z interference, lead to a further correction of -0.2% (-0.1%) on the value of A_b (A_c).

A list of systematic errors is shown in Table I. The purity of the separation of $Z^0 \rightarrow b\bar{b}$ and $Z^0 \rightarrow c\bar{c}$ events via secondary vertex information introduces an uncertainty dominated by the efficiency of charged track reconstruction, which has been constrained by reweighting MC tracks by the ratio of the number of tracks in data and MC as a function of p and p_t . The ability of the L/D variable to discriminate between bl and $b\bar{c}l$ decays is sensitive to the fraction of $B \rightarrow D\bar{D}$ decays, which has been constrained from SLD data [18].

For the 1996-98 muon sample, we find that $A_b = 0.938 \pm 0.044(\text{stat.}) \pm 0.024(\text{syst.})$ and $A_c = 0.560 \pm 0.063(\text{stat.}) \pm 0.064(\text{syst.})$, with a statistical correlation coefficient of 0.108. For the corresponding electron sample, we find $A_b = 0.896 \pm 0.050(\text{stat.}) \pm 0.028(\text{syst.})$. Combined with the result of [2], we find overall SLD average results via semileptonic B and D hadron decay of

$$A_b = 0.919 \pm 0.030(\text{stat.}) \pm 0.024(\text{syst.})$$

$$A_c = 0.583 \pm 0.055(\text{stat.}) \pm 0.055(\text{syst.}).$$

In conclusion, we have directly measured the extent of parity violation in the coupling of Z^0 bosons to b and c quarks using identified charged leptons from semileptonic decays. The results presented here take advantage of an additional sample of 400000 Z^0 decays, and employ a new method of signal source separation, resulting in substantial increases in precision

relative to previous measurements [2]. These results are in agreement with the Standard Model predictions $A_b = 0.935$ and $A_c = 0.667$, which are insensitive to uncertainties in Standard Model parameters such as the strong and electromagnetic coupling strengths, and the top quark and Higgs boson masses.

We thank the staff of the SLAC accelerator department for their outstanding efforts on our behalf. This work was supported by the U.S. Department of Energy and National Science Foundation, the UK Particle Physics and Astronomy Research Council, the Istituto Nazionale di Fisica Nucleare of Italy and the Japan-US Cooperative Research Project on High Energy Physics.

REFERENCES

- [1] The LEP collaborations and the LEP electroweak working group, CERN-EP/99-15 and CERN-PPE/97-154 and references therein.
- [2] K. Abe *et al.*, *Phys. Rev. Lett.* **83**, 3384 (1999).
- [3] K. Abe *et al.*, *Nucl. Instr. & Meth.* **A400**, 287 (1997).
- [4] K. Abe *et al.*, *Phys. Rev. Lett.* **78**, 2075 (1997).
- [5] K. Abe *et al.*, *Phys. Rev.* **D53**, 1023 (1996).
- [6] W. Bartel *et al.*, *Z. Phys.* **C33**, 23 (1986).
- [7] D. Jackson, *Nucl. Instr. & Meth.* **A388**, 247 (1997).
- [8] K. Abe *et al.*, *Phys. Rev. Lett.* **80**, 660 (1998).
- [9] J. P. Fernandez, Ph.D. Thesis, SCIPP 99/57, December 1999.
- [10] K. Abe *et al.*, *Phys. Rev. Lett.* **84**, 4300 (2000).
- [11] T. Sjöstrand *et al.*, *Comp. Phys. Comm.* **82**, 74 (1994).
- [12] N. Isgur, D. Scora, B. Grinstein, M. Wise, *Phys. Rev.* **D39**, 799 (1989); code provided by P. Kim and CLEO Collaboration.
- [13] Review of Particle Properties, *Phys. Rev.* **D50**, 1173 (1994).
- [14] B. Barish *et al.*, *Phys. Rev. Lett.* **76**, 1570 (1996); L. Gibbons *et al.*, *Phys. Rev.* **D56**, 2783 (1997).
- [15] M. Thulasidas, PhD thesis, Syracuse University (1993).
- [16] W. Bacino *et al.*, *Phys. Rev. Lett.* **43**, 1073 (1979).
- [17] GEANT 3.21 program, CERN Applications Software Group, CERN Program Library.
- [18] G. Bellodi, Ph.D. Thesis, SLAC-REPORT-566, February 2001.

- [19] J.B. Stav and H.A. Olsen, *Phys. Rev.* **D52**, 1359 (1995); *ibidem.*, *Phys. Rev.* **D50**, 6775 (1994); V. Ravindran and W.L. van Neerven, *Phys. Lett.* **B445**, 206 (1998); S. Catani, M. Seymour, *Journal of High Energy Physics*, 9907:023 (1999).
- [20] P. Abreu *et al.*, *Phys. Lett.* **B405**, 202 (1997); R. Barate *et al.*, *Phys. Lett.* **B434**, 437 (1998).
- [21] G. Altarelli *et al.*, *Nucl. Phys.* **B208**, 365 (1982).

FIGURES

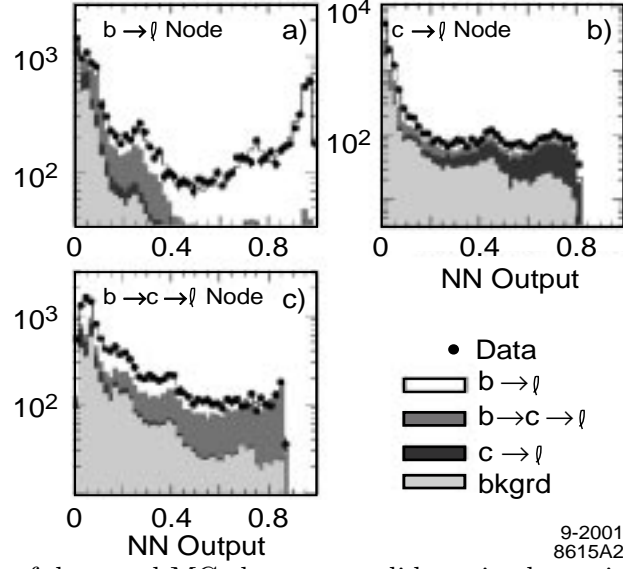


FIG. 1. Distribution of data and MC electron candidates in the various NN output node variables.

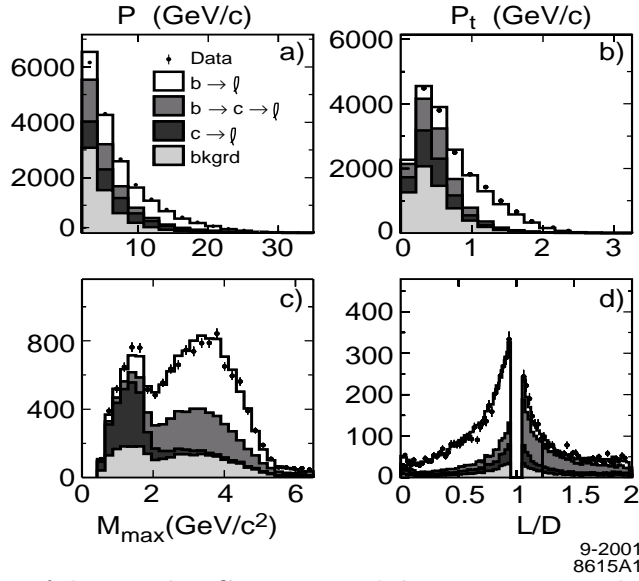


FIG. 2. Distributions of data and MC muon candidates. Events with L/D very close to 1 are suppressed in the L/D plot.

TABLES

| Source | Parameter variation | $\delta A_b(\mu)$ | $\delta A_b(e)$ | $\delta A_c(\mu)$ |
|--|---|-------------------|-----------------|-------------------|
| Monte Carlo statistics | Includes Neural Net training for e | $\pm.005$ | $\pm.014$ | $\pm.023$ |
| Jet axis simulation | 10 mrad smearing | $\pm.002$ | $\pm.006$ | $\pm.002$ |
| Background level | $\pm 10\%$ relative | $\pm.003$ | $\pm.004$ | $\pm.010$ |
| Background asymmetry | $\pm 40\%$ relative | $\mp.002$ | $\mp.003$ | $\pm.007$ |
| $\text{BR}(Z^0 \rightarrow b\bar{b})$ | $R_b = .2164 \pm .0007$ | $\mp.000$ | $\pm.000$ | $\pm.001$ |
| $\text{BR}(Z^0 \rightarrow c\bar{c})$ | $R_c = .1674 \pm .0038$ | $\pm.001$ | $\pm.000$ | $\mp.008$ |
| $\text{BR}(b \rightarrow l)$ | $(10.62 \pm 0.17)\%$ | $\mp.003$ | $\mp.003$ | $\pm.003$ |
| $\text{BR}(\bar{b} \rightarrow \bar{c} \rightarrow l)$ | $(8.07 \pm 0.25)\%$ | $\pm.003$ | $\pm.003$ | $\mp.003$ |
| $\text{BR}(b \rightarrow \bar{c} \rightarrow l)$ | $(1.62 \pm 0.40)\%$ | $\mp.006$ | $\mp.001$ | $\pm.011$ |
| $\text{BR}(b \rightarrow \tau \rightarrow l)$ | $(0.452 \pm 0.074)\%$ | $\mp.003$ | $\mp.001$ | $\mp.002$ |
| $\text{BR}(b \rightarrow J/\psi \rightarrow l)$ | $(0.07 \pm 0.02)\%$ | $\pm.003$ | $\pm.002$ | $\pm.000$ |
| $\text{BR}(\bar{c} \rightarrow l)$ | $(9.85 \pm 0.32)\%$ | $\pm.001$ | $\pm.001$ | $\mp.012$ |
| B lept. spect. - D^{**} fr. | $(23 \pm 10)\%$, B^+, B^0 ; $(32 \pm 10)\%$, B_s | $\pm.003$ | $\pm.002$ | $\pm.001$ |
| D lept. spect. | $ACCM1$ ($^{+ACCM2}$ / $^{-ACCM3}$) [21] | $\pm.004$ | $\pm.004$ | $\pm.002$ |
| B_s fraction in $b\bar{b}$ event | $.115 \pm .050$ | $\pm.001$ | $\pm.004$ | $\mp.001$ |
| Λ_b fraction in $b\bar{b}$ event | $.072 \pm .030$ | $\pm.002$ | $\pm.002$ | $\mp.001$ |
| b fragmentation | $\epsilon_b = .0045-.0075$ [11] | $\pm.001$ | $\pm.004$ | $\pm.002$ |
| c fragmentation | $\epsilon_c = .045-.070$ [11] | $\mp.003$ | $\mp.000$ | $\pm.012$ |
| Polarization | $\langle P_e \rangle = 73.4 \pm 0.4$ | $\mp.005$ | $\mp.005$ | $\mp.003$ |
| QCD Corrections | α_S , gluon splitting, selection bias | $\pm.005$ | $\pm.005$ | $\pm.005$ |
| Gluon Splitting | $g_{cc} = (2.33 \pm 0.50)\%$; $g_{bb} = (0.27 \pm 0.07)\%$ | $\pm.001$ | $\pm.001$ | $\pm.002$ |
| B mixing χ_b | $\chi = .1186 \pm .0043$ | $\pm.010$ | $\pm.011$ | $\pm.000$ |
| N_{D^0}/N_{D^+} in B Decay | $\pm 10\%$ | $\pm.002$ | $\pm.001$ | $\pm.003$ |
| B tag purity | Track efficiency | $\pm.012$ | $\pm.014$ | $\pm.053$ |
| L/D variable | Data/MC comparison | $\pm.002$ | $\pm.000$ | $\pm.005$ |

| | | | | |
|--|--------------------|-----------|-------------|-----------|
| Neural Net Training | | — | $\pm.013$ | — |
| $B \rightarrow D\bar{D} \rightarrow l$ | $(11.5 \pm 2.5)\%$ | $\pm.010$ | $\pm.008$ | $\pm.003$ |
| A_c | 0.667 ± 0.030 | — | ± 0.002 | — |
| Total Systematic | | $\pm.024$ | $\pm.028$ | $\pm.064$ |

TABLE I. Systematic errors

List of Figures

- 1 Distribution of data and MC electron candidates in the various NN output node variables. 10
- 2 Distributions of data and MC muon candidates. Events with L/D very close to 1 are suppressed in the L/D plot. 10

List of Tables

- I Systematic errors 12

** The SLD Collaboration

Kenji Abe,⁽¹⁵⁾ Koya Abe,⁽²⁴⁾ T. Abe,⁽²¹⁾ I. Adam,⁽²¹⁾ H. Akimoto,⁽²¹⁾ D. Aston,⁽²¹⁾
K.G. Baird,⁽¹¹⁾ C. Baltay,⁽³⁰⁾ H.R. Band,⁽²⁹⁾ T.L. Barklow,⁽²¹⁾ J.M. Bauer,⁽¹²⁾
G. Bellodi,⁽¹⁷⁾ R. Berger,⁽²¹⁾ G. Blaylock,⁽¹¹⁾ J.R. Bogart,⁽²¹⁾ G.R. Bower,⁽²¹⁾ J.E. Brau,⁽¹⁶⁾
M. Breidenbach,⁽²¹⁾ W.M. Bugg,⁽²³⁾ D. Burke,⁽²¹⁾ T.H. Burnett,⁽²⁸⁾ P.N. Burrows,⁽¹⁷⁾
A. Calcaterra,⁽⁸⁾ R. Cassell,⁽²¹⁾ A. Chou,⁽²¹⁾ H.O. Cohn,⁽²³⁾ J.A. Coller,⁽⁴⁾
M.R. Convery,⁽²¹⁾ V. Cook,⁽²⁸⁾ R.F. Cowan,⁽¹³⁾ G. Crawford,⁽²¹⁾ C.J.S. Damerell,⁽¹⁹⁾
M. Daoudi,⁽²¹⁾ N. de Groot,⁽²⁾ R. de Sangro,⁽⁸⁾ D.N. Dong,⁽²¹⁾ M. Doser,⁽²¹⁾ R. Dubois,⁽²¹⁾
I. Erofeeva,⁽¹⁴⁾ V. Eschenburg,⁽¹²⁾ S. Fahey,⁽⁵⁾ D. Falciari,⁽⁸⁾ J.P. Fernandez,⁽²⁶⁾
K. Flood,⁽¹¹⁾ R. Frey,⁽¹⁶⁾ E.L. Hart,⁽²³⁾ K. Hasuko,⁽²⁴⁾ S.S. Hertzbach,⁽¹¹⁾ M.E. Huffer,⁽²¹⁾
X. Huynh,⁽²¹⁾ M. Iwasaki,⁽¹⁶⁾ D.J. Jackson,⁽¹⁹⁾ P. Jacques,⁽²⁰⁾ J.A. Jaros,⁽²¹⁾ Z.Y. Jiang,⁽²¹⁾
A.S. Johnson,⁽²¹⁾ J.R. Johnson,⁽²⁹⁾ R. Kajikawa,⁽¹⁵⁾ M. Kaelkar,⁽²⁰⁾ H.J. Kang,⁽²⁰⁾
R.R. Kofler,⁽¹¹⁾ R.S. Kroeger,⁽¹²⁾ M. Langston,⁽¹⁶⁾ D.W.G. Leith,⁽²¹⁾ V. Lia,⁽¹³⁾ C. Lin,⁽¹¹⁾
G. Mancinelli,⁽²⁰⁾ S. Manly,⁽³⁰⁾ G. Mantovani,⁽¹⁸⁾ T.W. Markiewicz,⁽²¹⁾ T. Maruyama,⁽²¹⁾
A.K. McKemey,⁽³⁾ R. Messner,⁽²¹⁾ K.C. Moffeit,⁽²¹⁾ T.B. Moore,⁽³⁰⁾ M. Morii,⁽²¹⁾
D. Muller,⁽²¹⁾ V. Murzin,⁽¹⁴⁾ S. Narita,⁽²⁴⁾ U. Nauenberg,⁽⁵⁾ H. Neal,⁽³⁰⁾ G. Nesom,⁽¹⁷⁾
N. Oishi,⁽¹⁵⁾ D. Onoprienko,⁽²³⁾ L.S. Osborne,⁽¹³⁾ R.S. Panvini,⁽²⁷⁾ C.H. Park,⁽²²⁾
I. Peruzzi,⁽⁸⁾ M. Piccolo,⁽⁸⁾ L. Piemontese,⁽⁷⁾ R.J. Plano,⁽²⁰⁾ R. Prepost,⁽²⁹⁾
C.Y. Prescott,⁽²¹⁾ B.N. Ratcliff,⁽²¹⁾ J. Reidy,⁽¹²⁾ P.L. Reinertsen,⁽²⁶⁾ L.S. Rochester,⁽²¹⁾
P.C. Rowson,⁽²¹⁾ J.J. Russell,⁽²¹⁾ O.H. Saxton,⁽²¹⁾ T. Schalk,⁽²⁶⁾ B.A. Schumm,⁽²⁶⁾
J. Schwiening,⁽²¹⁾ V.V. Serbo,⁽²¹⁾ G. Shapiro,⁽¹⁰⁾ N.B. Sinev,⁽¹⁶⁾ J.A. Snyder,⁽³⁰⁾
H. Staengle,⁽⁶⁾ A. Stahl,⁽²¹⁾ P. Stamer,⁽²⁰⁾ H. Steiner,⁽¹⁰⁾ D. Su,⁽²¹⁾ F. Suekane,⁽²⁴⁾
A. Sugiyama,⁽¹⁵⁾ S. Suzuki,⁽¹⁵⁾ M. Swartz,⁽⁹⁾ F.E. Taylor,⁽¹³⁾ J. Thom,⁽²¹⁾ E. Torrence,⁽¹³⁾
T. Usher,⁽²¹⁾ J. Va'vra,⁽²¹⁾ R. Verdier,⁽¹³⁾ D.L. Wagner,⁽⁵⁾ A.P. Waite,⁽²¹⁾ S. Walston,⁽¹⁶⁾
A.W. Weidemann,⁽²³⁾ E.R. Weiss,⁽²⁸⁾ J.S. Whitaker,⁽⁴⁾ S.H. Williams,⁽²¹⁾ S. Willocq,⁽¹¹⁾
R.J. Wilson,⁽⁶⁾ W.J. Wisniewski,⁽²¹⁾ J.L. Wittlin,⁽¹¹⁾ M. Woods,⁽²¹⁾ T.R. Wright,⁽²⁹⁾
R.K. Yamamoto,⁽¹³⁾ J. Yashima,⁽²⁴⁾ S.J. Yellin,⁽²⁵⁾ C.C. Young,⁽²¹⁾ H. Yuta.⁽¹⁾

(The SLD Collaboration)

⁽¹⁾ *Aomori University, Aomori, 030 Japan,*

⁽²⁾ *University of Bristol, Bristol, United Kingdom,*

⁽³⁾ *Brunel University, Uxbridge, Middlesex, UB8 3PH United Kingdom,*

⁽⁴⁾ *Boston University, Boston, Massachusetts 02215,*

⁽⁵⁾ *University of Colorado, Boulder, Colorado 80309,*

⁽⁶⁾ *Colorado State University, Ft. Collins, Colorado 80523,*

⁽⁷⁾ *INFN Sezione di Ferrara and Università di Ferrara, I-44100 Ferrara, Italy,*

⁽⁸⁾ *INFN Lab. Nazionali di Frascati, I-00044 Frascati, Italy,*

- ⁽⁹⁾ *Johns Hopkins University, Baltimore, Maryland 21218-2686,*
⁽¹⁰⁾ *Lawrence Berkeley Laboratory, University of California, Berkeley, California 94720,*
⁽¹¹⁾ *University of Massachusetts, Amherst, Massachusetts 01003,*
⁽¹²⁾ *University of Mississippi, University, Mississippi 38677,*
⁽¹³⁾ *Massachusetts Institute of Technology, Cambridge, Massachusetts 02139,*
⁽¹⁴⁾ *Institute of Nuclear Physics, Moscow State University, 119899, Moscow Russia,*
⁽¹⁵⁾ *Nagoya University, Chikusa-ku, Nagoya, 464 Japan,*
⁽¹⁶⁾ *University of Oregon, Eugene, Oregon 97403,*
⁽¹⁷⁾ *Oxford University, Oxford, OX1 3RH, United Kingdom,*
⁽¹⁸⁾ *INFN Sezione di Perugia and Università di Perugia, I-06100 Perugia, Italy,*
⁽¹⁹⁾ *Rutherford Appleton Laboratory, Chilton, Didcot, Oxon OX11 0QX United Kingdom,*
⁽²⁰⁾ *Rutgers University, Piscataway, New Jersey 08855,*
⁽²¹⁾ *Stanford Linear Accelerator Center, Stanford University, Stanford, California 94309,*
⁽²²⁾ *Soongsil University, Seoul, Korea 156-743,*
⁽²³⁾ *University of Tennessee, Knoxville, Tennessee 37996,*
⁽²⁴⁾ *Tohoku University, Sendai 980, Japan,*
⁽²⁵⁾ *University of California at Santa Barbara, Santa Barbara, California 93106,*
⁽²⁶⁾ *University of California at Santa Cruz, Santa Cruz, California 95064,*
⁽²⁷⁾ *Vanderbilt University, Nashville, Tennessee 37235,*
⁽²⁸⁾ *University of Washington, Seattle, Washington 98105,*
⁽²⁹⁾ *University of Wisconsin, Madison, Wisconsin 53706,*
⁽³⁰⁾ *Yale University, New Haven, Connecticut 06511.*

*Deceased